Title

Adsorption Thermodynamics and Intrinsic Activation Parameters for Monomolecular Cracking of n-Alkanes on Brønsted Acid Sites in Zeolites

Journal

The Journal of Physical Chemistry C, 119(19)

ISSN

1932-7447

Authors

Janda, Amber
Vlaisavljevich, Bess
Lin, Li-Chiang
et al.

Publication Date

2015-05-14

DOI

10.1021/acs.jpcc.5b01715

Peer reviewed

THE JOURNAL OF PHYSICAL CHEMISTRY C

Article

pubs.acs.org/JPCC

Adsorption Thermodynamics and Intrinsic Activation Parameters for Monomolecular Cracking of *n*-Alkanes on Brønsted Acid Sites in Zeolites

Amber Janda,[†] Bess Vlaisavljevich,[†] Li-Chiang Lin,[†,§] Shaama Mallikarjun Sharada,[†] Berend Smit,[†,⊥] Martin Head-Gordon,[‡] and Alexis T. Bell*[,†]

[†]Department of Chemical and Biomolecular Engineering and [‡]Department of Chemistry, University of California, Berkeley, Berkeley, California 94720, United States

[§]Department of Process and Energy, Delft University of Technology, Leeghwaterstraat 39, 2628CB Delft, The Netherlands

[⊥]Institut des Sciences et Ingénierie Chimiques, Ecole Polytechnique Fédérale de Lausanne (EPFL), CH-1015 Lausanne, Switzerland

Supporting Information

ABSTRACT: Experimental measurements of the rate coefficient (k_{app}) and apparent enthalpies and entropies of activation (ΔH_{app} and ΔS_{app}) for alkane cracking catalyzed by acidic zeolites can be used to characterize the effects of zeolite structure and alkane size on the intrinsic enthalpy and entropy of activation, $\Delta H^{\ddagger}_{int}$ and $\Delta S^{\ddagger}_{int}$. To determine $\Delta H^{\ddagger}_{int}$ and $\Delta S^{\ddagger}_{int}$, enthalpies and entropies of adsorption, $\Delta H_{ads\text{-}H^+}$ and $\Delta S_{ads\text{-}H^+}$, must be determined for alkane molecules moving from the gas phase to Brønsted acid sites at reaction temperatures (>673 K). Experimental values of ΔH_{app} and ΔS_{app} must also be properly defined in terms of $\Delta H_{ads\text{-}H^+}$ and $\Delta S_{ads\text{-}H^+}$. We report here a method for determining $\Delta H_{ads\text{-}H^+}$ and $\Delta S_{ads\text{-}H^+}$ in which the adsorption site is represented by a fixed volume that includes the proton. Values of $\Delta H_{ads\text{-}H^+}$ and $\Delta S_{ads\text{-}H^+}$ obtained from Monte Carlo simulations are in good agreement with values obtained from experimental data measured at 300−400 K. An important feature of the simulations, however, is their ability to account for the redistribution of alkane adsorbed at protons in different locations with increasing temperature. Values of $\Delta H^{\ddagger}_{int}$ and $\Delta S^{\ddagger}_{int}$ for the cracking of propane through *n*-hexane, determined from measured values of k_{app} and ΔH_{app} and simulated values of $\Delta H_{ads\text{-}H^+}$ and $\Delta S_{ads\text{-}H^+}$, agree well with values obtained independently from quantum mechanics/molecular mechanics calculations. Application of our method of analysis reveals that the observed increase in k_{app} with increasing *n*-alkane size is due primarily to a decrease in $\Delta H^{\ddagger}_{int}$ with increasing chain length and that $\Delta S^{\ddagger}_{int}$ is independent of chain length.

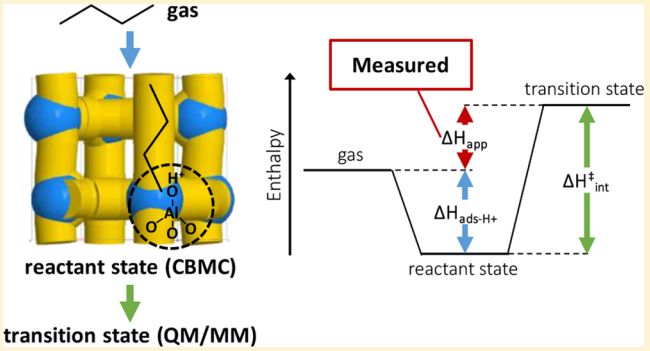

1. INTRODUCTION

The cracking of alkanes catalyzed by Brønsted acid centers in zeolites has been investigated extensively given the impact of this process on the conversion of petroleum to transportation fuels.[1] Studies of alkane cracking kinetics have demonstrated that at high conversion cracking occurs via a bimolecular chain propagation mechanism, whereas at very low conversion and low partial pressure a monomolecular pathway dominates whereby alkane molecules are converted into products by direct interaction with Brønsted protons.[2,3] The latter mechanism has been shown to be first order in alkane partial pressure and is not limited by the diffusion of reactant molecules to active sites for small alkanes and for crystal sizes typical of those used as cracking catalysts.[4−6] For these reasons monomolecular alkane cracking can be used to probe the influences of zeolite structure (pore size and topology) on the intrinsic activity and selectivity of Brønsted acid sites for the cracking of alkane C−C bonds. To make such an analysis, it is necessary to relate the intrinsic activation barriers to the experimentally measured values, which are influenced by the thermodynamics of alkane adsorption as well as the intrinsic kinetics. In this study we propose a rigorous basis for relating the thermodynamics of alkane adsorption to the intrinsic activation enthalpy and entropy for cracking.

We begin our presentation by developing an approach for determining $\Delta H_{ads\text{-}H^+}$ and $\Delta S_{ads\text{-}H^+}$, the enthalpy and entropy changes for alkane molecules moving from the gas phase to a Brønsted acid site (a reactant state) within a zeolite using Monte Carlo simulations. Values of $\Delta H_{ads\text{-}H^+}$ and $\Delta S_{ads\text{-}H^+}$ obtained from simulations are in good agreement with experiment at the temperatures of the adsorption measurements, and at higher temperatures our approach properly

Received: February 20, 2015
Revised: April 10, 2015
Published: April 17, 2015

DOI: 10.1021/acs.jpcc.5b01715
J. Phys. Chem. C 2015, 119, 10427−10438

captures the effects of the redistribution of alkane to different parts of the zeolite.

The values of $\Delta H_{ads\text{-}H^+}$ and $\Delta S_{ads\text{-}H^+}$ obtained from simulation are then used to extract the intrinsic enthalpy and entropy of activation, $\Delta H^{\ddagger}_{int}$ and $\Delta S^{\ddagger}_{int}$, from the apparent enthalpy and entropy of activation, ΔH_{app} and ΔS_{app}, determined from experimental activation energies and rate coefficients measured at 773 K for propane through *n*-hexane. Values of $\Delta H^{\ddagger}_{int}$ and $\Delta S^{\ddagger}_{int}$ obtained through the use of simulated values of $\Delta H_{ads\text{-}H^+}$ and $\Delta S_{ads\text{-}H^+}$ at 773 K are consistent with those determined independently from quantum chemical calculations. We also show that the increase in the apparent rate coefficient for alkane cracking with increasing chain length observed experimentally is due primarily to a decrease in $\Delta H^{\ddagger}_{int}$ and that $\Delta S^{\ddagger}_{int}$ varies little with chain length.

2. THEORETICAL APPROACH FOR DETERMINING ADSORPTION THERMODYNAMICS AND INTRINSIC ACTIVATION PARAMETERS

Alkane unimolecular cracking in zeolites occurs via the direct activation of an alkane C−C bond by a zeolitic proton and proceeds through a charged transition state that decomposes into a smaller alkane and an alkene.[7−10] The elementary steps of adsorption and reaction that occur in this process are presented in Scheme 1.[11,12]

Scheme 1. Steps Involved in the Monomolecular Cracking of Alkane Molecules in Acidic Zeolites: (1) Adsorption of Gas Phase Alkane, A_g, into the Zeolite Pores, and (2) Cracking of Alkane Molecules Located in a Reactant State at Brønsted Protons, $A_{z,react}$

1. $A_g \rightleftharpoons A_z$
2. $A_{z,react} \rightleftharpoons [TS] \rightarrow$ Products

Step 1 describes the adsorption of gas phase alkane (A_g) into the zeolite pores to give adsorbed alkane (A_z). The adsorbed molecules can be located anywhere within the pores (near Brønsted protons or at siliceous parts of the framework), and at low loadings of the adsorbate the number of molecules adsorbed per unit mass of zeolite is proportional to the Henry coefficient (K_H) and the alkane pressure (P_A). A fraction of the adsorbed molecules, given by P_{react} (discussed below), is located sufficiently close to a Brønsted proton to initiate a reaction ($[A_{z,react}] = P_{react}\cdot[A_z]$). Such molecules are considered to be in a "reactant state" and may undergo cracking in step 2. Because diffusion does not usually limit the rates of monomolecular cracking,[6] it is assumed that alkane molecules in the gas phase are in quasi-equilibrium with molecules in a reactant state and that the rate-determining step is the cracking of $A_{z,react}$. The apparent rate of reaction, r, can be represented as the product of the intrinsic rate coefficient for cracking, k_{int}, and the fraction of Brønsted acid sites occupied by alkane molecules, $\theta_{A_{z,react}}$:

$$r = k_{int}\theta_{A_{z,react}} \tag{1}$$

At the high temperatures and low conversions of monomolecular cracking, it can be further assumed that $\theta_{A_{z,react}}$ is much less than 1 and is therefore proportional to P_A.[12,13] This assumption is consistent with the empirical observation of a first-order dependence of r on P_A

$$r = k_{app}P_A \tag{2}$$

where k_{app} is the apparent first-order rate coefficient for cracking.

To interpret the influence of the zeolite structure on measured cracking rates, it is useful to separate the apparent reaction barriers determined from an Arrhenius plot of k_{app} into contributions from adsorption thermodynamics (contained in $\theta_{A_{z,react}}$) and intrinsic reaction barriers (contained in k_{int}).[12−14] To perform such an analysis, $\theta_{A_{z,react}}$ must be related to the alkane partial pressure and to enthalpies and entropies of adsorption for the transfer of alkane molecules from the gas phase to the Brønsted protons ($\Delta H_{ads\text{-}H^+}$ and $\Delta S_{ads\text{-}H^+}$). Following Swisher et al.,[11] we express $\theta_{A_{z,react}}$ when the site coverage is very low ($\theta_{A_{z,react}} \ll 1$) as

$$\theta_{A_{z,react}} = \frac{P_{react}}{n_{H^+}}K_H P_A \tag{3}$$

In this equation, K_H is Henry's constant (mol kg^{-1} Pa^{-1}) for adsorption from the gas into the zeolite pores (step 1 of Scheme 1), n_{H^+} is the number of Brønsted acid sites per unit mass of zeolite (mol kg^{-1}), and P_{react} is the (dimensionless) probability that a molecule adsorbed in the zeolite is in a reactant state. These authors have used geometrical arguments to define the reactant state ($A_{z,react}$) as any configuration in which an alkane C−C bond is located within 5 Å of a zeolite Al atom. By substituting the above expression for $\theta_{A_{z,react}}$ into eq 1 and setting the result equal to the rate expression given by eq 2, k_{app} can be written

$$k_{app} = \frac{P_{react}}{n_{H^+}}K_H k_{int} \tag{4}$$

Swisher et al.[11] have shown that both P_{react} and K_H can be obtained from Monte Carlo simulations over a broad range of temperatures for silicalite, the all-silica form of the zeolite MFI, and Tranca et al.[15] have shown that the same methods can be used to obtain K_H for MFI with one Al atom (one Brønsted proton) per unit cell. However, before data from such simulations can be used, P_{react} and K_H must be defined in terms of $\Delta H_{ads\text{-}H^+}$ and $\Delta S_{ads\text{-}H^+}$.

We begin by defining the Henry coefficient in accordance with Swisher et al.[11] and Tranca et al.[15] as

$$K_H \equiv \frac{1}{\rho_f RT}\exp\left(-\frac{\Delta A_{ads}}{RT}\right) \tag{5}$$

where ρ_f is the zeolite framework density and ΔA_{ads} is the Helmholtz free energy for adsorption into the zeolite. We note that the Helmholtz free energy (and not the Gibbs free energy) is a natural thermodynamic function for gas adsorption into a solid adsorbent.[16] The value of ΔA_{ads} represents an ensemble average for adsorption at protons and at nonacidic parts of the zeolite and depends on both the zeolite Si/Al ratio and the crystallographic location of the Al atoms. The significance of this latter point is discussed below.

As shown in the Supporting Information (section S.1), an expression can be written for P_{react}, defined as the ratio of alkane molecules adsorbed at protons ($A_{z,react}$) to alkane molecules adsorbed anywhere in the zeolite (A_z):

DOI: 10.1021/acs.jpcc.5b01715
J. Phys. Chem. C 2015, 119, 10427−10438

$$P_{\text{react}} = f_{H^+} \exp\left(-\frac{\Delta A_{\text{react}}}{RT}\right) = f_{H^+} \exp\left(-\frac{\Delta U_{\text{react}} - T\Delta S_{\text{react}}}{RT}\right) \quad (6)$$

where f_{H^+} is the fraction of the zeolite volume that is contained within 5 Å of an Al atom. The differences in the Helmholtz energy, internal energy, and entropy between alkane adsorbed anywhere in the pores (A_z) and alkane located only in a reactant state ($A_{z,\text{react}}$) are denoted, respectively, by ΔA_{react}, ΔU_{react}, and ΔS_{react}. We define f_{H^+} as

$$f_{H^+} \equiv n_{H^+}\rho_f V_{H^+} \quad (7)$$

where V_{H^+} is the volume of 1 mol of reactant state spheres of radius 5 Å. Equation 7 gives the ratio of the volume of reactant state spheres to the total volume of the zeolite. We note that eq 6 can also be written as

$$p_{\text{react}} = \rho_f V_{H^+} \exp\left(-\frac{\Delta A_{\text{react}}}{RT}\right) \quad (8)$$

where we have substituted $p_{\text{react}} \equiv P_{\text{react}}/n_{H^+}$ after the nomenclature of Swisher et al.[11] The values of p_{react} and of ΔA_{react} depend weakly on the type of reactant state complex being formed (e.g., for central or terminal cracking) and to a larger extent on the local environment of the active site (the T site at which the Al atom is located).[11,12] As the number of Brønsted acid sites per unit mass of zeolite decreases ($f_{H^+} \to 0$), P_{react} approaches 0. In the limit of low f_{H^+}, ΔA_{react}, ΔU_{react}, and ΔS_{react} are equal to the differences in Helmholtz energy, internal energy, and entropy between alkane adsorbed only at the siliceous parts of the framework and alkane adsorbed only at Brønsted protons. The value of P_{react} is then proportional to n_{H^+}.

By combining the equations for p_{react} and K_H, the dimensionless equilibrium constant for adsorption from the gas phase onto active sites can be obtained:

$$K_{\text{ads-H}^+} = p_{\text{react}} K_H \frac{RT}{V_{H^+}} \equiv \exp\left(-\frac{\Delta A_{\text{ads-H}^+}}{RT}\right) \quad (9)$$

where $\Delta A_{\text{ads-H}^+}$ (equal to $\Delta U_{\text{ads-H}^+} - T\Delta S_{\text{ads-H}^+}$) is the Helmholtz free energy change for adsorption of alkane from the gas to a reactant state. In this work, values of p_{react}, $\Delta U_{\text{ads-H}^+}$, and K_H are obtained from simulations for MFI containing one Al per unit cell for each T site. The value of $\Delta S_{\text{ads-H}^+}$ is then determined using eq 9, recalling that $\Delta A_{\text{ads-H}^+} = \Delta U_{\text{ads-H}^+} - T\Delta S_{\text{ads-H}^+}$.

An expression for k_{app} can now be written in terms of thermodynamic adsorption parameters and intrinsic activation parameters. The expression for k_{int} is taken from absolute rate theory

$$k_{\text{int}} = \frac{k_B T}{h} \exp\left(-\frac{\Delta G^{\ddagger}_{\text{int}}}{RT}\right) \quad (10)$$

where $\Delta G^{\ddagger}_{\text{int}}$ is the intrinsic Gibbs energy barrier for the reaction. This expression and eqs 5−7 are substituted into eq 4 to give

$$k_{\text{app}} = \frac{v_{H^+}}{h} \exp\left(-\frac{\Delta A_{\text{ads-H}^+} + \Delta G^{\ddagger}_{\text{int}}}{RT}\right) \quad (11)$$

where v_{H^+} is the volume of one Al site (one sphere of radius 5 Å). Expressions for the apparent enthalpy and entropy of activation, ΔH_{app} and ΔS_{app}, can be written by first substituting the relationship $\Delta A_{\text{ads-H}^+} = \Delta U_{\text{ads-H}^+} - T\Delta S_{\text{ads-H}^+}$ into eq 11. The following expressions are then obtained that relate ΔH_{app} and ΔS_{app}, determined from an Arrhenius plot of k_{app}, to $\Delta H_{\text{ads-H}^+}$ and $\Delta S_{\text{ads-H}^+}$ and the intrinsic activation parameters:

$$\Delta H_{\text{app}} = \Delta H_{\text{ads-H}^+} + \Delta H^{\ddagger}_{\text{int}} = -R\left[\frac{\partial \ln k_{\text{app}}}{\partial(1/T)}\right] - RT \quad (12)$$

$$\Delta S_{\text{app}} = \Delta S_{\text{ads-H}^+} + \Delta S^{\ddagger}_{\text{int}} = R\left[\ln k_{\text{app},T\to\infty} - \ln \frac{v_{H^+}}{h}\right] \quad (13)$$

It should be noted that in eq 12, $\Delta U_{\text{ads-H}^+}$ has been substituted with the quantity $\Delta H_{\text{ads-H+}} + RT$. This relationship arises because ΔU_{ads} is obtained directly from the simulations, whereas ΔH_{ads} is obtained by subtracting RT from ΔU_{ads} to account for the work done on the system due to the volume change in the gas phase.[17−19] Equations 12 and 13 provide a quantitative basis for interpreting the influence of the zeolite structure on adsorption and intrinsic reaction steps, where $\Delta H_{\text{ads-H}^+}$ and $\Delta S_{\text{ads-H}^+}$ have been defined in a way that allows these quantities to be determined using Monte Carlo simulations.

In section 4 we compare values of $\Delta H_{\text{ads-H}^+}$ and $\Delta S_{\text{ads-H}^+}$ obtained from Monte Carlo simulations to values determined from experimental measurements. It is therefore necessary to first review how $\Delta H_{\text{ads-H}^+}$ and $\Delta S_{\text{ads-H}^+}$ are extracted from experimental data. Conventionally, it is assumed that the fraction of acid sites occupied by adsorbed alkane in a zeolite can be represented by a Langmuir isotherm:[13−22]

$$\theta_{A_{z,\text{react}}} = \frac{K_{\text{L-H}^+} P_A}{1 + K_{\text{L-H}^+} P_A} \quad (14)$$

where $K_{\text{L-H}^+}$ is the Langmuir constant for adsorption at Brønsted protons. In the limit of low site coverage occurring at the reaction temperatures of interest (>673 K), $\theta_{A_{z,\text{react}}}$ reduces to[13]

$$\theta_{A_{z,\text{react}}} = K_{\text{L-H}^+} P_A \quad (15)$$

A common approach used to define thermodynamic adsorption parameters in the context of alkane adsorption in zeolites is to define standard chemical potentials for the adsorbed and gaseous phases and require that these potentials are equal at equilibrium.[23−25] This treatment leads to a relationship between $K_{\text{L-H}^+}$ and the dimensionless thermodynamic equilibrium constant at standard conditions, $K^{\circ}_{\text{ads-H}^+}$,[23,26,27] given by

$$K^{\circ}_{\text{ads-H}^+} \equiv \exp\left(-\frac{\Delta G^{\circ}_{\text{ads-H}^+}}{RT}\right) = \frac{1-\theta^{\circ}}{\theta^{\circ}} P^{\circ} K_{\text{L-H}^+} \quad (16)$$

where θ° and P° are the standard states for the fractional coverage and the gas phase partial pressure, and $\Delta G^{\circ}_{\text{ads-H}^+}$ is the Gibbs free energy change for the transfer of molecules at pressure P° and temperature T to the adsorption sites, a fraction θ° of which are already occupied. The standard enthalpy and entropy of adsorption, $\Delta H^{\circ}_{\text{ads-H}^+}$ (kJ mol^{-1}) and $\Delta S^{\circ}_{\text{ads-H}^+}$ (J mol^{-1} K^{-1}), can then be obtained from the slope and

DOI: 10.1021/acs.jpcc.5b01715
J. Phys. Chem. C 2015, 119, 10427−10438

intercept of a van't Hoff plot[27] according to eqs 17, 18, or 19, respectively.

$$\Delta H^{\circ}_{\text{ads-H}^+} = -R\frac{\partial \ln K_{\text{L-H}^+}}{\partial(1/T)} \tag{17}$$

$$\Delta S^{\circ}_{\text{ads-H}^+} = R\left[\lim_{T\to\infty}(\ln P^{\circ}K_{\text{L-H}^+}) - \ln\left(\frac{\theta^{\circ}}{1-\theta^{\circ}}\right)\right] \tag{18}$$

$$\Delta S^{\circ}_{\text{ads-H}^+} = R\ln K^{\circ}_{\text{ads-H}^+} + \frac{\Delta H^{\circ}_{\text{ads-H}^+}}{T} \tag{19}$$

The value of $\Delta H^{\circ}_{\text{ads-H}^+}$ can also be measured calorimetrically if the adsorbed molecules are located only at Brønsted acid sites.[28] Eder et al.[21,22] and De Moor et al.[30] have reported such measurements made at 323 K and at 300−400 K, respectively, for several zeolites and alkanes. Specific adsorption of alkanes at Brønsted protons was verified by in situ infrared studies in combination with gravimetry and calorimetry. The value of $\Delta S^{\circ}_{\text{ads-H}^+}$ was then obtained by substituting the measured value of $\Delta H^{\circ}_{\text{ads-H}^+}$ into eq 19 after extraction of $K_{\text{L-H}^+}$ from a dual-site Langmuir isotherm, fit to the experimental data and accounting for adsorption at acidic and nonacidic sites. De Moor et al. have stated that there was little variation in the values of $\Delta H^{\circ}_{\text{ads-H}^+}$ and $\Delta S^{\circ}_{\text{ads-H}^+}$ over the temperature range 300−400 K and assumed, therefore, that these values are temperature independent even up to the temperature at which alkane cracking occurs. As discussed below, this assumption proves not to be correct because it does not account for the fact that with increasing temperature, the distribution of alkane in the reactant state at different Al T-sites changes because the values of $\Delta H_{\text{ads-H}^+}$ and $\Delta S_{\text{ads-H}^+}$ differ for different T-sites.

In this work we compare values of $\Delta H_{\text{ads-H}^+}$ and $\Delta S_{\text{ads-H}^+}$ obtained from simulation to values of $\Delta H^{\circ}_{\text{ads-H}^+}$ and $\Delta S^{\circ}_{\text{ads-H+}}$ taken from the literature. We then use both sets of values and eqs 12 and 13 to determine intrinsic activation parameters for *n*-alkane cracking. Before doing so, it is necessary to ensure that values of $\Delta S^{\circ}_{\text{ads-H}^+}$ reported in the literature have the same reference state as $\Delta S_{\text{ads-H}^+}$ obtained from simulation. It can be shown that (see Supporting Information, section S.2), although $\Delta H_{\text{ads-H}^+}$ and $\Delta H^{\circ}_{\text{ads-H}^+}$ are independent of the standard state pressure and adsorbate coverage, the following equation adjusts the reference state of $\Delta S^{\circ}_{\text{ads-H}^+}$ to match that of $\Delta S_{\text{ads-H}^+}$:

$$\Delta S_{\text{ads-H}^+} = \Delta S^{\circ}_{\text{ads-H}^+} + R\left[\ln\left(\frac{\theta^{\circ}}{1-\theta^{\circ}}\right) - \ln\left(\frac{P^{\circ}V_{\text{H}^+}}{RT}\right) + 1\right] \tag{20}$$

3. METHODS

3.1. Configurational-Bias Monte Carlo (CBMC) Simulations. CBMC simulations were performed following the approach described by Swisher et al.[11] and Tranca et al.[15] A Lennard-Jones-type potential using the force field parameters of Dubbeldam et al.[17,29] (included in the Supporting Information, section S.8) was employed to describe the interaction between the zeolite and the linear alkanes propane through *n*-hexane, whereas the TraPPE potential was used to describe the guest.[31] Alkane molecules were treated using the united atom approach for the methyl ($-CH_3$) and methylene ($-CH_2-$) groups. These groups were connected with harmonic bonds, bending angles, and torsions. For longer chains, internal van der Waals interactions were also included. The atoms comprising the zeolite were fixed at the experimental crystallographic positions reported by van Koningsveld et al.,[32] included in the Supporting Information (section S.8). In addition, to model the Brønsted acid site, the oxygen parameters were modified[11,15] to reflect the stronger interaction of alkane molecules with Brønsted protons relative to the siliceous parts of the framework (i.e., Eder and Lercher[33] have measured a difference of ∼10 kJ mol^{-1} for the heat of adsorption of *n*-hexane in H-MFI relative to silicalite). For each T-site, a simulation was performed treating one of the four oxygen atoms bonded to the T-site as the one to which the proton is bonded.

The Henry coefficient, K_H, and the enthalpy of adsorption, $\Delta H_{ads} = \Delta U_{ads} - RT$, were computed for H-MFI with one Al (one Brønsted proton) per unit cell using the Widom particle insertion method at temperatures spanning 278−773 K. Although we do not analyze values of ΔH_{ads} explicitly in this work, it is important to note that our simulated values of ΔH_{ads} are identical to those reported by Tranca et al.[15] and are, therefore, in good agreement with the experimentally measured isosteric heats of adsorption reported in ref 33.

Additionally, the probability of finding an alkane molecule in the reactant state (P_{react}) and the enthalpy of adsorption from the gas phase to the reactant state, $\Delta H_{\text{ads-H}^+} = \Delta U_{\text{ads-H}^+} - RT$, were computed by performing CBMC simulations in an NVT ensemble for a single alkane molecule. Values of $P_{react}(i,j)$ and $\Delta H_{\text{ads-H}^+}(i,j)$ were computed for each individual C−C bond *j* located within a 5.0 Å radius of T-site *i* as described in ref 11. We demonstrate in the Supporting Information (section S.6) that this cutoff radius is similar to the Al−C distances calculated from DFT for *n*-alkanes adsorbed at Brønsted protons in H-MFI and is also consistent with the geometric parameters reported by Jiang et al.[34] for molecular dynamics simulations of alkanes interacting with Brønsted protons in CHA. On the basis of our analysis of the sensitivity of $\Delta H_{\text{ads-H}^+}$ and $\Delta S_{\text{ads-H}^+}$ to the choice of the cutoff radius, we estimate that the uncertainties in these values for each alkane at fixed temperature are ∼2 kJ mol^{-1} and ∼10 J mol^{-1} K^{-1}, respectively. The values of $\Delta H_{\text{ads-H}^+}(i,j)$ were determined from the ensemble average energy of reactant states involving bond *j* located within 5.0 Å of T-site *i* and the corresponding values of $\Delta S_{\text{ads-H}^+}(i,j)$ determined using eq 9. A Boltzmann weighted average of $\Delta H_{\text{ads-H}^+}(i)$ over all bonds *j* was performed to determine the values of $\Delta H_{\text{ads-H}^+}$ for adsorption of the molecule at T-site *i*.

3.2. Density Functional Theory (DFT). The cluster model for representing the MFI zeolite framework consisted of 437 tetrahedral (T) atoms and was terminated with hydrogen atoms. Adapting an approach similar to our previous work,[35] calculations were performed for the active site located in the channel intersection (T12, O24). This location was chosen for the Al to enable comparison of our results with previous theoretical studies of alkane cracking in MFI in which the active site was located at T12.[11,15,35,36] The quantum mechanics/molecular mechanics (QM/MM) method developed by Zimmerman et al.[37] was used employing Lennard-Jones parameters for framework Si and O atoms adapted from more recent work.[38] Accordingly, the zeolite model was divided into two regions: a T5 cluster containing the active site was treated quantum mechanically and the remaining T432 cluster treated classically.

All calculations were performed using a developmental version of the Q-Chem software package.[39] Geometry optimizations and vibrational analyses were carried out using the dispersion-corrected, range-separated hybrid density func-

DOI: 10.1021/acs.jpcc.5b01715
J. Phys. Chem. C 2015, 119, 10427−10438

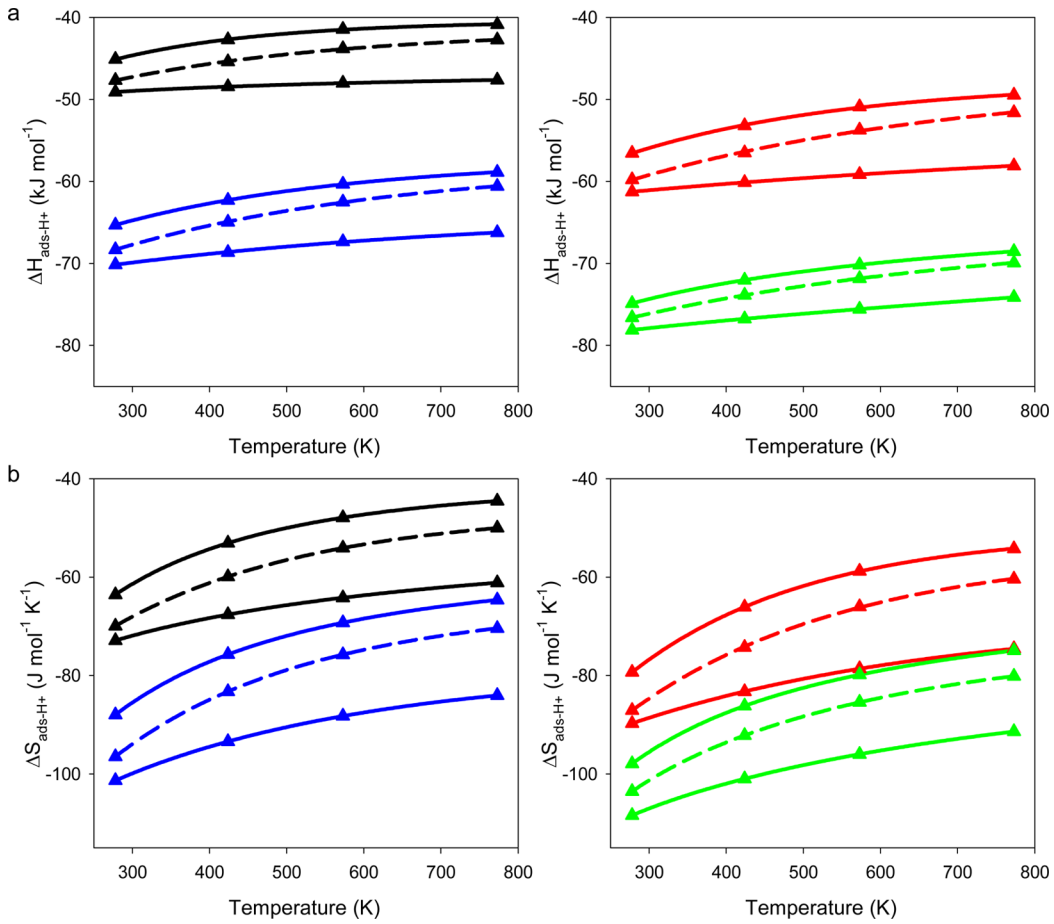

Figure 1. Plots of (a) enthalpy changes $\Delta H_{ads\text{-}H^+}$ and (b) entropy changes $\Delta S_{ads\text{-}H^+}$ for the adsorption of propane (black triangles) and *n*-pentane (blue triangles) (left) and of *n*-butane (red triangles) and *n*-hexane (green triangles) (right) from the gas phase onto Brønsted protons in H-MFI with one Al per unit cell obtained using CBMC simulations. The upper and lower solid lines correspond to Al located only at T9 and T4, respectively. The dashed lines represent the Boltzmann weighted averages of $\Delta H_{ads\text{-}H^+}$ and $\Delta S_{ads\text{-}H^+}$ for Al distributed evenly between T9 and T4.

tional, ωB97X-D,[40,41] and a triple-ζ polarized basis set, 6-311G**.[42] Transition state guesses were obtained using a double-ended interpolation technique known as the freezing string method (FSM)[43,44] and further refined using partitioned-rational function optimization (P-RFO).[45] Transition states were determined for central and terminal cracking of *n*-butane. These transition states correspond to TS1 in our previous theoretical work.[35]

Zero-point energies were added to ground-state electronic energies. To calculate intrinsic activation energies and entropies at the reaction temperature of 773 K, thermodynamic corrections to the ground state were computed. The rigid rotor/harmonic oscillator (RRHO) approximation is the most commonly used technique. However, entropies calculated in zeolite-based systems using this method are typically inaccurate owing to the presence of several soft modes in the vibrational spectrum.[46,47] Because these modes are better treated as internal rotations, a composite hindered rotor approach proposed by Grimme[48] was employed. This technique allows for smooth interpolation between a free rotor at lower frequencies and a harmonic oscillator at higher frequencies using a frequency-dependent weighting function. The average molecular moment of inertia, B_{av}, was modified from the original work to be equal to the average of free rotor moments of inertia over all frequencies. In addition, the weighting function parameter, ω_0, was chosen to be 268 cm^{-1} on the basis of the criteria proposed by Grimme.[48]

A similar procedure was employed to calculate enthalpies and entropies of adsorption for the linear alkanes propane through *n*-hexane adsorbed at a Brønsted proton associated with site T12, O24 in MFI at 773 K. Earlier investigations have demonstrated that the assumption of an immobile adsorbate results in the overestimation of entropy losses on adsorption.[30] Therefore, two simple possibilities were explored. In the first case, the adsorbate can translate, but not rotate, in the vicinity of the adsorption site. In the second case, the adsorbate cannot translate but retains its gas phase rotational degrees of freedom upon adsorption. To determine the entropy of translation for the first scenario, the largest included sphere diameter of 6.3 Å reported by Foster et al.[49] for MFI was used. The value of $\Delta S^{\circ}_{ads\text{-}H^+}$ returned by QM/MM calculations was then adjusted using eq 20 before comparison with values of $\Delta S_{ads\text{-}H^+}$ determined from Monte Carlo simulations. The standard configurational entropy term appearing in eq 20, given by

$$\Delta S^{\circ}_{config} = -R \ln\left(\frac{\theta^{\circ}}{1-\theta^{\circ}}\right) \tag{21}$$

was set equal to zero because the QM/MM calculations involve only one adsorption site,[27,28,50] and the standard state pressure P° was set equal to 10^5 Pa, the pressure employed in the QM/MM calculations.

DOI: 10.1021/acs.jpcc.5b01715
J. Phys. Chem. C 2015, 119, 10427−10438

4. RESULTS AND DISCUSSION

4.1. Dependences of $\Delta H_{ads\text{-}H^+}$ and $\Delta S_{ads\text{-}H^+}$ on Al Siting and Temperature. Figure 1 shows the effects of temperature on the values of $\Delta H_{ads\text{-}H^+}$ and $\Delta S_{ads\text{-}H^+}$ for propane, *n*-butane, *n*-pentane, and *n*-hexane determined from Monte Carlo simulations for MFI containing one Al atom per unit cell at either T9 (upper solid curves) or T4 (lower solid curves). Site T9 resides near the intersection of the straight and sinusoidal channels, whereas T4 is located on the wall of the sinusoidal channel (see Figure S.6 of ref 12). Sites T9 and T4 were chosen from the 12 possible T-sites because the magnitudes of $\Delta H_{ads\text{-}H^+}$ and $\Delta S_{ads\text{-}H^+}$ are usually the smallest (T9) and largest (T4) for these sites. (Individual values of $\Delta H_{ads\text{-}H^+}$, $\Delta S_{ads\text{-}H^+}$, p_{react}, and K_H for each T-site are tabulated in the Supporting Information, section S.7.)

The increase of $\Delta H_{ads\text{-}H+}$ with temperature is consistent with the molecular dynamics (MD) simulations of Bučko et al.[9] and Jiang et al.,[34] who observed that alkane molecules in a reactant state (molecules that interact directly with a Brønsted proton) lie farther from the proton at higher temperatures than at lower temperatures. Although the reactant state is still defined by a 5 Å radius surrounding an Al atom, at higher temperatures molecules within this radius adopt configurations that are farther from the proton than at lower temperatures, causing a decrease in the magnitude of $\Delta H_{ads\text{-}H^+}$. Similar effects are responsible for the increase in $\Delta S_{ads\text{-}H^+}$ with temperature seen in Figure 1b, although part of the increase in $\Delta S_{ads\text{-}H^+}$ with temperature is caused by the appearance of the temperature T on the left-hand side of eq 9. Figure 1 also shows that $\Delta H_{ads\text{-}H^+}$ and $\Delta S_{ads\text{-}H^+}$ are more negative for T4 than for T9, consistent with the smaller size of the channels (where T4 is located) relative to the intersection (where T9 is located), and the commensurately stronger van der Waals interactions between the zeolite walls and the alkane.[51] It is interesting to note that the spread between the curves for T9 and T4 in Figure 1 is smallest for *n*-hexane, consistent with the greater number of ways that the smaller *n*-alkanes may orient within the MFI pores.[19,52,53]

When Al is situated in more than one type of pore environment (e.g., channels and intersections), the temperature variations of $\Delta H_{ads\text{-}H^+}$ and $\Delta S_{ads\text{-}H^+}$ are also influenced by changes in the locations at which molecules adsorb with increasing temperature. The dashed curves shown in Figure 1 correspond to values of $\Delta H_{ads\text{-}H^+}$ and $\Delta S_{ads\text{-}H^+}$ for a zeolite with Al distributed evenly between sites T9 and T4. These curves give the probability-weighted Boltzmann average of $\Delta H_{ads\text{-}H^+}$ and $\Delta S_{ads\text{-}H^+}$ (see Supporting Information, section S.3). At the lowest temperature (278 K), the values of $\Delta H_{ads\text{-}H^+}$ and $\Delta S_{ads\text{-}H^+}$ for MFI containing Al in both T9 and T4 sites (the dashed curves) are closer to those for T4, whereas at higher temperatures they are closer to those for T9. It is also evident that the magnitudes of these changes are different for each alkane.

Contributing to the temperature variation of the dashed curves of Figure 1 are changes in the probabilities for localization of the adsorbate at T9 and T4 with temperature. At higher temperatures molecules are more likely to adsorb at protons associated with Al atoms in intersections (T9) because the entropy loss for adsorption at the intersections is smaller than for adsorption at protons located in the sinusoidal channel (T4),[51] which is preferred at lower temperature due to the higher enthalpic stabilization at this location.[54] This behavior is confirmed by a plot of the ratio of $K_{ads\text{-}H^+}$ (calculated using eq 9) for adsorption at T9 relative to that for T4 versus temperature, shown in Figure 2. At 773 K, molecules are more likely to reside at T9 than at T4, whereas at 278 K molecules are more likely to adsorb at T4. As a consequence, at lower temperatures the ensemble-average values of $\Delta H_{ads\text{-}H^+}$ and $\Delta S_{ads\text{-}H^+}$ (the dashed lines of Figure 1) are closer to the solid curves for T4, and at higher temperature the dashed lines are closer to the solid curves for T9.

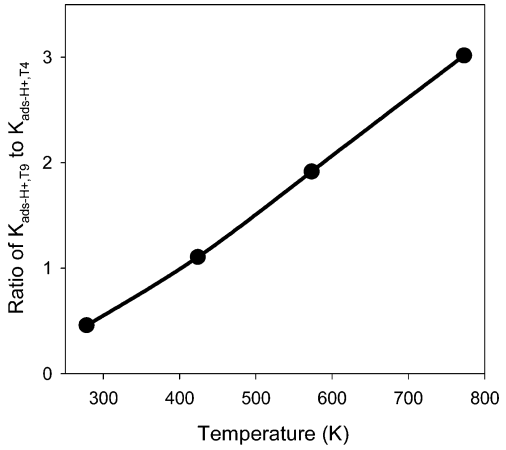

Figure 2. Ratio of equilibrium constant ($K_{ads\text{-}H^+}$) for *n*-butane adsorption at site T9 relative to that for adsorption at site T4 as a function of temperature.

The preceding analysis demonstrates that changes in $\Delta H_{ads\text{-}H^+}$ and $\Delta S_{ads\text{-}H^+}$ with temperature are larger when Al is distributed over multiple T-sites than when Al is located at only one type of T-site. These effects are more pronounced for smaller alkanes (<C6) because the spread among values of $\Delta H_{ads\text{-}H^+}$ and $\Delta S_{ads\text{-}H^+}$ for adsorption at different T-sites is greater for these alkanes, which may orient in a greater variety of ways relative to *n*-hexane, as noted above. This raises the issue of how, in general, the distribution of Al atoms among different framework T-sites affects the ensemble-average values of $\Delta H_{ads\text{-}H^+}$ and $\Delta S_{ads\text{-}H^+}$[50,56] and the dependences of these values on temperature and alkane size.

Whereas the effects of structural heterogeneity on $\Delta H_{ads\text{-}H^+}$ and $\Delta S_{ads\text{-}H^+}$ are modest for MFI, such effects will be more significant for zeolites with more variegated pore structures, such as MWW, because of the known correlation of pore size with $\Delta H_{ads\text{-}H^+}$. For example, at ambient temperature alkanes are found to adsorb preferentially in the 10-MR sinusoidal channels of MWW.[57] On the basis of the increasing preference for adsorption in less confining locations with increasing temperature noted above,[54] at higher temperatures molecules will adsorb with greater preference for the supercages of MWW, thereby causing the ensemble average values of $\Delta H_{ads\text{-}H^+}$ and $\Delta S_{ads\text{-}H^+}$ to become less negative[55] and the incremental changes in $\Delta H_{ads\text{-}H^+}$ and $\Delta S_{ads\text{-}H^+}$ with respect to *n*-alkane chain length to become smaller.[19,22,33]

The next task is to compare values of $\Delta H_{ads\text{-}H^+}$ and $\Delta S_{ads\text{-}H^+}$ obtained from Monte Carlo simulations with those obtained from experimental data. Because the experimental data are collected using an MFI sample having an unknown distribution of Al, the simulated values of $\Delta H_{ads\text{-}H^+}$ and $\Delta S_{ads\text{-}H^+}$ were obtained by calculating a Boltzmann weighted average of $\Delta H_{ads\text{-}H^+}$ and $\Delta S_{ads\text{-}H^+}$ for the 12 T-sites obtained from Monte

DOI: 10.1021/acs.jpcc.5b01715
J. Phys. Chem. C 2015, 119, 10427−10438

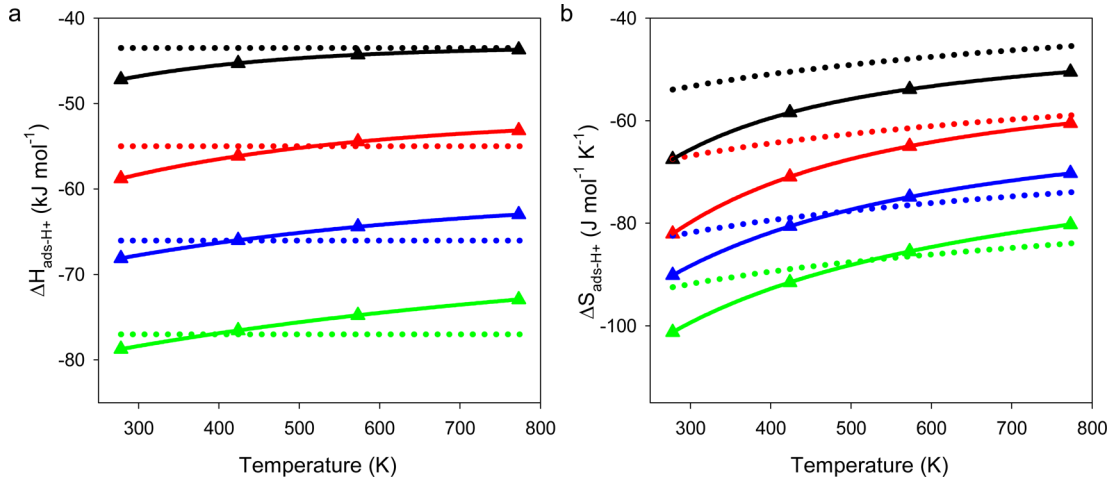

Figure 3. Plots of the Boltzmann weighted average enthalpy ($\Delta H_{ads\text{-}H^+}$) and entropy changes ($\Delta S_{ads\text{-}H^+}$) for adsorption of propane (black triangles), *n*-butane (red triangles), *n*-pentane (blue triangles), and *n*-hexane (green triangles) from the gas phase onto Brønsted protons in H-MFI with a random distribution of Al, obtained using CBMC simulations. The dashed lines represent the averages of experimental values reported by Eder et al.[22] and by De Moor et al.,[30] measured at 323 K and at 300−400 K, respectively, and extrapolated to 278−773 K.

Carlo simulations (corresponding to a random distribution of Al). These values of $\Delta H_{ads\text{-}H^+}$ and $\Delta S_{ads\text{-}H^+}$ are now compared with those obtained from experiments. The experimental values were taken from Eder et al.[22] (for 323 K) and from De Moor et al.[30] (for 300−400 K). De Moor et al. state that they have employed the same zeolite sample and the same methods of measurement as Eder et al. and that the measured heat of adsorption did not vary significantly between 300 and 400 K. In our discussion we have used the average values of $\Delta H^{o}_{ads\text{-}H^+}$ and $\Delta S^{o}_{ads\text{-}H^+}$ reported in these two studies.

Values of $\Delta H_{ads\text{-}H^+}$ and $\Delta S_{ads\text{-}H^+}$ determined from Monte Carlo simulations and the averaged experimental values of $\Delta H_{ads\text{-}H^+}$ (equivalent to $\Delta H^{o}_{ads\text{-}H^+}$) and $\Delta S_{ads\text{-}H^+}$ (determined using eq 20 and the experimentally measured value of $\Delta S^{o}_{ads\text{-}H+}$) are presented as solid and dashed lines, respectively, in Figure 3. We should note that $\Delta H^{o}_{ads\text{-}H^+}$ and $\Delta S^{o}_{ads\text{-}H^+}$ for adsorption from the gas to a given type of acid site are expected to increase with temperature because of the increase in the specific heat of the alkane upon adsorption.[20] Previous authors[30,20] have estimated that these changes are small between 300 and 800 K, and our simulation data also show that this increase is usually small (≤14%), but depends on the alkane size and T-site (see Supporting Information, section S.4). Without a rigorous basis for calculating changes in $\Delta H^{o}_{ads\text{-}H^+}$ and $\Delta S^{o}_{ads\text{-}H^+}$ with temperature, we have neglected such effects in our analysis. For this reason, the experimental values of $\Delta H_{ads\text{-}H^+}$ (Figure 3a) are shown as independent of temperature, whereas the experimental values of $\Delta S_{ads\text{-}H^+}$ (Figure 3b) change with temperature only because of the temperature-dependent term appearing in eq 20.

It can be seen from Figure 3 that at the temperatures of the adsorption measurements (300−400 K), the values of $\Delta H_{ads\text{-}H^+}$ and $\Delta S_{ads\text{-}H^+}$ obtained by Monte Carlo simulations and the average of the values obtained from experiment are in reasonable agreement, although the experimental values of $\Delta H_{ads\text{-}H^+}$ and $\Delta S_{ads\text{-}H^+}$ are systematically less negative than the simulated values. Although this observation could be related to uncertainties in the force field parameters and cutoff radius, we note that exact agreement of the experimental and simulated values of $\Delta H_{ads\text{-}H^+}$ and $\Delta S_{ads\text{-}H^+}$ is not expected because the distribution of Al in the experimental sample is unknown. It is therefore interesting to note that the experimental values of $\Delta H_{ads\text{-}H^+}$ and $\Delta S_{ads\text{-}H^+}$ shown in Figure 3 (at the temperature of the adsorption measurements) are closer to the values of $\Delta H_{ads\text{-}H^+}$ and $\Delta S_{ads\text{-}H^+}$ at the same temperature for site T9, shown in Figure 1. This observation suggests that the Al in the MFI sample used for the adsorption measurements may be located primarily at T-sites that are relatively unconfined, such as site T9. This hypothesis is consistent with spectroscopic studies that have demonstrated that the distribution of Al in MFI is nonrandom and depends on the synthesis conditions.[58−66] It can also be seen that the temperature variations of both $\Delta H_{ads\text{-}H^+}$ and $\Delta S_{ads\text{-}H^+}$ are stronger for the simulated values than for the values obtained from experiment. This observation is a result of the effects of temperature on the sites at which molecules adsorb and on the average distances of alkanes in a reactant state to Brønsted protons, as discussed above. Such effects are not captured by the approximation that the measured values of $\Delta H^{o}_{ads\text{-}H^+}$ and $\Delta S^{o}_{ads\text{-}H^+}$ are temperature independent.

4.2. Intrinsic Enthalpies and Entropies of Activation.

Having addressed the issue of how to determine $\Delta H_{ads\text{-}H^+}$ and $\Delta S_{ads\text{-}H^+}$ at temperatures at which monomolecular alkane cracking occurs, we proceed to use these values to extract intrinsic enthalpies and entropies of activation from experimentally measured rate data for *n*-alkane cracking. For this analysis we used the experimentally measured activation energies and rate coefficients reported by Narbeshuber et al.[67] for the cracking of propane through *n*-hexane at 773 K on H-MFI with a Si/Al ratio of 35. We note that the zeolite sample used by these authors was stated to be the same as that used for the adsorption measurements of Eder et al.[22] and De Moor et al.[30] The values of $\Delta H^{\ddagger}_{int}$ and $\Delta S^{\ddagger}_{int}$ for the rate of cracking per C−C bond were then determined using eqs 11−13, together with values of $\Delta H_{ads\text{-}H^+}$ and $\Delta S_{ads\text{-}H^+}$ presented in section 2 and obtained either from simulations at 773 K for a random distribution of Al or from experimental measurements at 323 K[22] and at 300−400 K.[30] We note that the experimentally measured activation energies, obtained from a slope of an Arrhenius plot, have first been converted into values of ΔH_{app} using eq 12.

DOI: 10.1021/acs.jpcc.5b01715
J. Phys. Chem. C 2015, 119, 10427−10438

Table 1. Values of $\Delta S_{ads\text{-}H^+}$ and $\Delta S^{\ddagger}_{int}$ (J mol^{-1} K^{-1}) for *n*-Alkane Adsorption and Cracking in MFI

	Eder et al.[22a]		De Moor et al.[30a]		simulation		QM/MM	
alkane	$\Delta S_{ads\text{-}H^+}$	$\Delta S^{\ddagger}_{int}$	$\Delta S_{ads\text{-}H^+}$	$\Delta S^{\ddagger}_{int}$	$\Delta S_{ads\text{-}H^+}$[b]	$\Delta S^{\ddagger}_{int}$	$\Delta S_{ads\text{-}H^+}$[c]	$\Delta S^{\ddagger}_{int}$[d]
propane	−49	−22	−41	−30	−51	−21	−39, −52 (−47)	−16
n-butane	−66	−19	−51	−34	−61	−25	−48, −57 (−56)	−10
n-pentane	−82	−11	−65	−28	−70	−23	−56, −62 (−67)	−7
n-hexane	−99	−5	−68	−36	−80	−24	−58, −61 (−78)	−10

[a]Values of $\Delta S_{ads\text{-}H^+}$ were obtained experimentally at 323 K[22] and between 300 and 400 K[30] or from CBMC simulations at 773 K. Values of $\Delta S^{\ddagger}_{int}$ were calculated by using these values of $\Delta S_{ads\text{-}H^+}$ and the rate coefficients and apparent activation enthalpies reported in ref 67. [b]Boltzmann weighted average value of $\Delta S_{ads\text{-}H^+}$ corresponding to a random distribution of Al. [c]Corresponds to adsorption at site T12. First and second values listed correspond to adsorption with local translation or rotation, respectively. CBMC value for T12 is given in parentheses. [d]Boltzmann weighted average intrinsic activation enthalpies for *n*-alkane cracking at 773 K in H-MFI at site T12.

Table 2. Values of $\Delta H_{ads\text{-}H^+}$ and $\Delta H^{\ddagger}_{int}$ (kJ mol^{-1}) for *n*-Alkane Adsorption and Cracking in MFI

	Eder et al.[22a]		De Moor et al.[30a]		simulation		QM/MM	
alkane	$\Delta H_{ads\text{-}H^+}$	$\Delta H^{\ddagger}_{int}$	$\Delta H_{ads\text{-}H^+}$	$\Delta H^{\ddagger}_{int}$	$\Delta H_{ads\text{-}H^+}$[b]	$\Delta H^{\ddagger}_{int}$	$\Delta H_{ads\text{-}H^+}$[c]	$\Delta H^{\ddagger}_{int}$[d]
propane	−46	194	−41	190	−44	192	−50 (−44)	182
n-butane	−58	187	−52	181	−53	182	−52 (−54)	184
n-pentane	−70	183	−63	176	−63	177	−60 (−64)	171
n-hexane	−82	182	−72	171	−73	171	−70 (−75)	172

[a]Values of $\Delta H_{ads\text{-}H^+}$ were obtained experimentally at 323 K[22] and between 300 and 400 K[30] or from CBMC simulations at 773 K. Values of $\Delta H^{\ddagger}_{int}$ were calculated by using these values of $\Delta H_{ads\text{-}H^+}$ and apparent activation enthalpies reported in ref 67. [b]Boltzmann weighted average value of $\Delta H_{ads\text{-}H^+}$ corresponding to a random distribution of Al. [c]Adsorption at site T12. CBMC value for T12 is given in parentheses. [d]Boltzmann weighted average intrinsic activation entropies for *n*-alkane cracking at 773 K in H-MFI at site T12.

Tables 1 and 2 present the values of $\Delta S^{\ddagger}_{int}$ and $\Delta H^{\ddagger}_{int}$ for each *n*-alkane using the different sets of values for $\Delta H_{ads\text{-}H^+}$ and $\Delta S_{ads\text{-}H^+}$. Values of $\Delta H^{\ddagger}_{int}$ and $\Delta S^{\ddagger}_{int}$ for cracking at site T12, and values of $\Delta H_{ads\text{-}H^+}$ and $\Delta S_{ads\text{-}H^+}$ corresponding to different degrees of rotational and translational freedom for adsorption at T12, calculated using QM/MM, are given in the last column on the right side of each table. These values for $\Delta H^{\ddagger}_{int}$ and $\Delta S^{\ddagger}_{int}$ represent a Boltzmann weighted average for cracking at each C−C bond (values of $\Delta H^{\ddagger}_{int}$ and $\Delta S^{\ddagger}_{int}$ for cracking at individual C−C bonds are included in the Supporting Information, section S.5). Also included in Tables 1 and 2 are the experimental and simulated values of $\Delta H_{ads\text{-}H^+}$ and $\Delta S_{ads\text{-}H^+}$ that were used to obtain $\Delta H^{\ddagger}_{int}$ and $\Delta S^{\ddagger}_{int}$ from the measured activation barriers.

Values of $\Delta H^{\ddagger}_{int}$ and $\Delta S^{\ddagger}_{int}$ determined using $\Delta H_{ads\text{-}H^+}$ and $\Delta S_{ads\text{-}H^+}$ obtained from Monte Carlo simulations at 773 K generally lie between the values obtained by using the adsorption data of De Moor et al.[30] and Eder et al.,[22] whereas the dependences of $\Delta H^{\ddagger}_{int}$ and $\Delta S^{\ddagger}_{int}$ on carbon number more closely reflect those that result from using the data of De Moor et al. We also note that the values of $\Delta H^{\ddagger}_{int}$ and the dependence of $\Delta H^{\ddagger}_{int}$ on chain length calculated using QM/MM are generally in closer agreement with those determined using the simulated adsorption data or those of De Moor et al. The lack of systematic variation of $\Delta S^{\ddagger}_{int}$ with alkane chain length obtained using QM/MM agrees well with the dependence of $\Delta S^{\ddagger}_{int}$ that results from using $\Delta S_{ads\text{-}H^+}$ obtained from Monte Carlo simulations or the adsorption data of De Moor et al., although the absolute values of $\Delta S^{\ddagger}_{int}$ obtained from QM/MM are less negative than the former sets of values.

It can also be seen that $\Delta H_{ads\text{-}H^+}$ and $\Delta S_{ads\text{-}H^+}$ determined using QM/MM for adsorption at T12 at 773 K generally agree with simulated values for adsorption at T12 (given in parentheses next to the QM/MM values in Tables 1 and 2) with the exception of $\Delta S_{ads\text{-}H^+}$ for *n*-pentane and *n*-hexane, for which QM/MM predicts a lower magnitude for $\Delta S_{ads\text{-}H^+}$. The latter values are less negative than those obtained from simulation or from experimental measurements, most likely as a consequence of the methods used to estimate the translational and rotational entropy of the adsorbate. We conclude on the basis of this analysis that the values of $\Delta H_{ads\text{-}H^+}$ and $\Delta S_{ads\text{-}H^+}$ obtained from Monte Carlo simulations are physically meaningful. Moreover, we suggest that this method be used to determine these quantities for high temperatures because it naturally accounts for the effects of temperature on the distribution of adsorbate molecules among Brønsted acid sites located in different regions (e.g., channels and pores) of the zeolite and on the different orientations that reactant state alkane molecules can adopt[34] at higher temperatures.

We next examine the changes in $\Delta H^{\ddagger}_{int}$ and $\Delta S^{\ddagger}_{int}$ with alkane chain length and the influence of these changes on the apparent and intrinsic rates of cracking. It can be seen from Tables 1 and 2 that $\Delta H^{\ddagger}_{int}$ decreases with the size of the alkane regardless of the adsorption data set used to determine $\Delta H^{\ddagger}_{int}$ from ΔH_{app}. These observations are consistent with the fact that QM/MM values of $\Delta H^{\ddagger}_{int}$ for cracking tend to be larger for shorter alkanes (C3 and C4) than for longer alkanes (C5 and C6). By contrast, the values of $\Delta S^{\ddagger}_{int}$ increase with chain length when using the data of Eder et al.,[22] but decrease or remain similar to increasing chain length using the adsorption data of De Moor et al.[30] or the values of $\Delta S_{ads\text{-}H^+}$ obtained from Monte Carlo simulations. The observed changes in $\Delta S^{\ddagger}_{int}$ with alkane size obtained by using the latter two sets of values for $\Delta S_{ads\text{-}H^+}$ are consistent with the observation that $\Delta S^{\ddagger}_{int}$ obtained using QM/MM varies little with the chain length.

The next issue that we address is the effect of alkane chain length on the rate coefficient for cracking. The apparent rate coefficients and activation energies (E_{app}) for cracking (per C−C bond) reported by Narbeshuber et al.[67] are presented in Table 3, along with the values of ΔH_{app} and ΔS_{app} determined using these quantities and eqs 12 and 13. It can be seen that k_{app} increases by a factor of ∼50 between propane and *n*-hexane

DOI: 10.1021/acs.jpcc.5b01715
J. Phys. Chem. C 2015, 119, 10427−10438

Table 3. Apparent Rate Coefficient per C−C Bond, k_{app} (s^{-1} bar^{-1}), and Activation Energies for Overall Cracking, E_{app} (kJ mol^{-1}), Reported in Reference 67, and Apparent Activation Enthalpies ΔH_{app} (kJ mol^{-1}) and Entropies ΔS_{app} (J mol^{-1} K^{-1}) Determined Using Equations 12 and 13

alkane	$k_{app} \times 10^2$	E_{app} [a]	ΔH_{app} [b]	ΔS_{app} [b]
propane	0.13	155	149	−72
n-butane	0.58	135	129	−85
n-pentane	2.2	120	114	−93
n-hexane	6.0	105	99	−104

[a] $E_{app} = -R\,\partial(\ln k_{app})/\partial T^{-1}$. [b] ΔH_{app} and ΔS_{app} obtained using eqs 12 and 13, respectively, and values of k_{app} and E_{app} summarized in this table.

as a result of a decrease in E_{app} with increasing chain size. We now note that k_{app} can be written by solving for the exponential terms in eqs 9 and 10 and then substituting these terms into eq 11 to give

$$k_{app} = \frac{V_{H^+}}{RT} k_{int} K_{ads\text{-}H^+} \tag{22}$$

Equation 22 shows that k_{app} is proportional to both the intrinsic rate coefficient and the equilibrium constant for adsorption to a reactant state. Therefore, the question is whether the observed increase in k_{app} is due primarily to changes in k_{int} or in $K_{ads\text{-}H^+}$ with increasing chain length. Table 4 shows the variations in k_{int} determined from eq 10 and the different sets of values for $\Delta H^{\ddagger}_{int}$ and $\Delta S^{\ddagger}_{int}$ discussed above. It is evident that, regardless of the methods used to determine $\Delta H^{\ddagger}_{int}$ and $\Delta S^{\ddagger}_{int}$, k_{int} increases with increasing chain length and is the principal cause for the increase in k_{app}. Values of $K_{ads\text{-}H^+}$ calculated using the different sets of values for $\Delta H_{ads\text{-}H^+}$ and $\Delta S_{ads\text{-}H^+}$ included in Tables 1 and 2 are given in Table 5. It can be seen that the remainder of the increase in k_{app} is due to larger values of $K_{ads\text{-}H^+}$ for larger alkanes, with the exception of the $K_{ads\text{-}H^+}$ values obtained using the adsorption data of Eder et al.,[22] which do not vary significantly with alkane size.

The final question to address is whether the variation in k_{int} with chain length is driven by changes in $\Delta H^{\ddagger}_{int}$ or $\Delta S^{\ddagger}_{int}$. The values of k_{int} shown in Table 4 depend in each case on $\Delta H^{\ddagger}_{int}$ and $\Delta S^{\ddagger}_{int}$, which in turn depend on the means by which $\Delta H_{ads\text{-}H^+}$ and $\Delta S_{ads\text{-}H^+}$ are determined. If the latter quantities are obtained from Monte Carlo simulations at 773 K or from QM/MM calculations, then $\Delta S^{\ddagger}_{int}$ is nearly invariant and $\Delta H^{\ddagger}_{int}$ is in general lower for longer *n*-alkanes. This observation indicates that the evaluation of $\Delta H_{ads\text{-}H^+}$ and $\Delta S_{ads\text{-}H^+}$ from Monte Carlo simulations results in physically meaningful dependences of these quantities on alkane chain length. A similar conclusion is reached if $\Delta H^{\ddagger}_{int}$ and $\Delta S^{\ddagger}_{int}$ are calculated using values of $\Delta H_{ads\text{-}H^+}$ and $\Delta S_{ads\text{-}H^+}$ (at 300−400 K) reported by De Moor et al.[30]

We note that a different conclusion regarding the effects of chain length on $\Delta H^{\ddagger}_{int}$ and $\Delta S^{\ddagger}_{int}$ is reached if these quantities are calculated using values of $\Delta H_{ads\text{-}H^+}$ and $\Delta S_{ads\text{-}H^+}$ (at 323 K) reported by Eder et al.[22] Tables 1 and 2 show that in this case, a major cause for the increase in k_{int} with alkane chain length is the increase of $\Delta S^{\ddagger}_{int}$ with alkane chain length. This conclusion is identical to that reported by Bhan et al.[20] These authors extracted $\Delta S^{\ddagger}_{int}$ from the measured rates and activation energies of Narbeshuber et al.[67] by first using the values of $\Delta H_{ads\text{-}H^+}$ and $\Delta S_{ads\text{-}H^+}$ (at 323 K) reported by Eder et al. to calculate an equilibrium constant for adsorption to extract k_{int} from k_{app}. Values of $\Delta H^{\ddagger}_{int}$ reported in ref 67 were then substituted into eq 14 to obtain $\Delta S^{\ddagger}_{int}$. This method of treating the data resulted in an increase in $\Delta S^{\ddagger}_{int}$ with carbon number, albeit stronger than that shown in Table 1. Bhan et al. attributed the increase in $\Delta S^{\ddagger}_{int}$ with chain length to an increase in the translational and rotational entropy of product fragments at the transition state with increasing alkane size.[20,68] The values of $\Delta H^{\ddagger}_{int}$ reported by Narbeshuber et al. and employed in the analysis of Bhan et al. are independent of alkane size. Tranca et al.[15] have also reported an increase in $\Delta S^{\ddagger}_{int}$ with respect to chain length. In this case, values of ΔH_{ads} and ΔS_{ads} obtained from Monte Carlo simulations for MFI with one Al atom per unit cell at 773 K were used in combination with the values of $\Delta H^{\ddagger}_{int}$ reported by Narbeshuber et al. to extract values of $\Delta S^{\ddagger}_{int}$. We note that the values of ΔH_{ads} and ΔS_{ads} reported by Tranca et al. correspond to adsorption anywhere in the zeolite and not only within 5 Å of an Al atom, the definition for adsorption into the reactant state used in the present study to determine values of $\Delta H_{ads\text{-}H^+}$ and $\Delta S_{ads\text{-}H^+}$ by Monte Carlo simulations.

The preceding discussion demonstrates that the variations in $\Delta H^{\ddagger}_{int}$ and $\Delta S^{\ddagger}_{int}$ with alkane chain length determined using experimental adsorption data are sensitive to the manner in which $\Delta H_{ads\text{-}H^+}$ and $\Delta S_{ads\text{-}H^+}$ are measured. Our work indicates that the evaluation of $\Delta H_{ads\text{-}H^+}$ and $\Delta S_{ads\text{-}H^+}$ from Monte Carlo simulations gives physically meaningful values, which when used to determine $\Delta H^{\ddagger}_{int}$ and $\Delta S^{\ddagger}_{int}$ lead to dependences of these quantities on alkane chain length that are consistent with independent QM/MM calculations. Therefore, we recommend that this approach be used to extract values of $\Delta H^{\ddagger}_{int}$ and $\Delta S^{\ddagger}_{int}$ from experimentally measured values of k_{app} measured as a function of temperature to determine the effects of hydrocarbon and zeolite structure on $\Delta H^{\ddagger}_{int}$ and $\Delta S^{\ddagger}_{int}$.

Although the present discussion has been framed on an analysis of intrinsic activation parameters for MFI, the use of simulated values of $\Delta H_{ads\text{-}H^+}$ and $\Delta S_{ads\text{-}H^+}$ to obtain $\Delta H^{\ddagger}_{int}$ and $\Delta S^{\ddagger}_{int}$ from experimentally measured activation barriers can readily be extended to other zeolites. A particular feature of the

Table 4. Apparent Rate Coefficient per C−C Bond, k_{app}, for *n*-Alkane Cracking in H-MFI at 773 K[67] and Intrinsic Rate Coefficients k_{int}, Calculated Using the Intrinsic Activation Parameters Given in Table 2 and by Using DFT

		k_{int} (s^{-1})[a]			
alkane	$k_{app} \times 10^2$ (s^{-1} bar^{-1})[a]	Eder et al.[22]	De Moor et al.[30]	simulation	QM/MM[b]
propane	0.13 (1)	0.09 (1)	0.07 (1)	0.13 (1)	1.3 (1)
n-butane	0.58 (4)	0.42 (5)	0.18 (3)	0.44 (3)	1.7 (1.3)
n-pentane	2.2 (17)	2.0 (23)	0.72 (11)	1.2 (9)	18 (15)
n-hexane	6.0 (46)	4.7 (54)	0.63 (9)	2.2 (17)	12 (10)

[a] Values in parentheses give the rate coefficient relative to propane. [b] Boltzmann weighted average rate of cracking per C−C bond at 773 K in H-MFI at site T12.

DOI: 10.1021/acs.jpcc.5b01715
J. Phys. Chem. C 2015, 119, 10427−10438

Table 5. Dimensionless Thermodynamic Equilibrium Constant, $K_{ads\text{-}H^+}$, for the Adsorption of *n*-Alkanes in MFI at 773 K

				QM/MM	
alkane	Eder et al.[22a]	De Moor et al.[30a]	simulation[a]	translation[b]	rotation[b]
propane	3.0 (1)	4.0 (1)	2.1 (1)	21 (1)	4.3 (1)
n-butane	2.8 (0.9)	6.7 (1.7)	2.7 (1.3)	9.6 (0.5)	3.2 (0.7)
n-pentane	2.3 (0.7)	6.4 (1.6)	3.8 (1.9)	13 (0.6)	6.2 (1.4)
n-hexane	2.6 (0.9)	19 (5)	5.4 (3)	47 (2)	33 (8)

[a]Calculated using eq 9 and the values of $\Delta H_{ads\text{-}H^+}$ and $\Delta S_{ads\text{-}H^+}$ given in Tables 1 and 2. [b]$K_{ads\text{-}H^+}$ values corresponding to local translation or rotation were calculated using the first or second QM/MM values of $\Delta S_{ads\text{-}H^+}$, respectively, presented in Table 1.

Monte Carlo simulation, as noted above, is its ability to represent correctly the relocation of adsorbate to active sites located within different parts of the zeolite pore volume (channels and cages). This relocation affects the values of $\Delta H_{ads\text{-}H^+}$ and $\Delta S_{ads\text{-}H^+}$[55] and their variation with chain length. The nature of this variation in turn affects the interpretation of how $\Delta H^{\ddagger}_{int}$ and $\Delta S^{\ddagger}_{int}$ depend on alkane size. For example, at room temperature, longer *n*-alkanes adsorb primarily at straight channels in MFI.[19,52] As the temperature increases, molecules distribute preferentially to the intersections,[54] and as a consequence of this relocation to less confining environments, the incremental changes in $\Delta H_{ads\text{-}H^+}$ and $\Delta S_{ads\text{-}H^+}$ with increasing carbon number are smaller.[19,22,33] Therefore, trends in $\Delta H^{\ddagger}_{int}$ and $\Delta S^{\ddagger}_{int}$ with respect to carbon number are different if values of $\Delta H_{ads\text{-}H^+}$ and $\Delta S_{ads\text{-}H^+}$ corresponding to ambient temperature are used instead of values corresponding to temperatures of cracking catalysis. As discussed in section 2, these effects will be more pronounced for zeolites with more heterogeneous pore systems (e.g., MWW).

5. CONCLUSIONS

A model has been developed for predicting the thermodynamics of alkane adsorption from the gas phase into a reactant state at Brønsted acid sites at low coverage in a zeolite. The active site is defined by the accessible volume contained in a sphere of 5 Å radius centered on a framework Al atom, and an alkane molecule is defined as being in the reactant state if one of its C−C bonds lies within this volume. Monte Carlo simulations are carried out to determine the enthalpies and entropies of adsorption into the reactant state, $\Delta H_{ads\text{-}H^+}$ and $\Delta S_{ads\text{-}H^+}$. The approach developed in this study accounts for changes with increasing temperature in the distribution of alkane molecules among active sites located in different portions of the zeolite pore space (channels and cages) and in the orientations that molecules adopt when in the reactant state at a given active site. The values of $\Delta H_{ads\text{-}H^+}$ and $\Delta S_{ads\text{-}H^+}$ at 300−400 K determined for MFI by Monte Carlo simulation are consistent with the average values of $\Delta H_{ads\text{-}H^+}$ and $\Delta S_{ads\text{-}H^+}$ determined from experimental measurements made for the same temperatures. It is also found that simulated values of $\Delta H_{ads\text{-}H^+}$ and $\Delta S_{ads\text{-}H^+}$ for adsorption at T12 agree well with those determined from quantum chemical calculations for adsorption at the same location.

We have also derived expressions for relating the apparent activation barriers for monomolecular alkane cracking at Brønsted acid sites, ΔH_{app} and ΔS_{app}, to the corresponding intrinsic barriers, $\Delta H^{\ddagger}_{int}$ and $\Delta S^{\ddagger}_{int}$, and to $\Delta H_{ads\text{-}H^+}$ and $\Delta S_{ads\text{-}H^+}$. We find that $\Delta H^{\ddagger}_{int}$ and $\Delta S^{\ddagger}_{int}$ for the cracking of propane through *n*-hexane in MFI at 773 K, extracted using simulated values of $\Delta H_{ads\text{-}H^+}$ and $\Delta S_{ads\text{-}H^+}$ at 773 K, agree with the values of $\Delta H^{\ddagger}_{int}$ and $\Delta S^{\ddagger}_{int}$ determined from quantum chemical calculations. The changes in these quantities with respect to increasing alkane size obtained using simulated values of $\Delta H_{ads\text{-}H^+}$ and $\Delta S_{ads\text{-}H^+}$ are also in agreement with those that are found using QM/MM. Reasonable agreement of values of $\Delta H^{\ddagger}_{int}$ and $\Delta S^{\ddagger}_{int}$, extracted using simulated values of $\Delta H_{ads\text{-}H^+}$ and $\Delta S_{ads\text{-}H^+}$ at 773 K, is found with those determined by using experimental values of $\Delta H_{ads\text{-}H^+}$ and $\Delta S_{ads\text{-}H^+}$ measured at lower temperatures. However, this agreement depends on which experimental data are chosen for $\Delta H_{ads\text{-}H^+}$ and $\Delta S_{ads\text{-}H^+}$, which were reported for different temperature ranges by different authors (i.e., 323 K[22] versus 300−400 K[30]). Experimentally measured values of $\Delta H_{ads\text{-}H^+}$ and $\Delta S_{ads\text{-}H^+}$ extrapolated to higher temperatures (773 K) do not reflect the redistribution of alkane to different parts of the zeolite (channels versus intersections) and, therefore, values of $\Delta H^{\ddagger}_{int}$ and $\Delta S^{\ddagger}_{int}$ obtained by subtracting measured values of $\Delta H_{ads\text{-}H^+}$ and $\Delta S_{ads\text{-}H^+}$ from ΔH_{app} and ΔS_{app} should be interpreted with caution.

Our analysis of the experimentally observed increase in the apparent rate coefficient for *n*-alkane cracking with increasing chain length in MFI indicates that most of this trend is due to the increase in the intrinsic rate coefficient and, to a lesser extent, the increase in the corresponding equilibrium constant for adsorption into the reactant state. We find that the intrinsic rate coefficient for cracking increases with chain length primarily because of a decrease in $\Delta H^{\ddagger}_{int}$, whereas $\Delta S^{\ddagger}_{int}$ is relatively insensitive to chain length.

■ ASSOCIATED CONTENT

Supporting Information

Values of K_H, p_{react}, $\Delta H_{ads\text{-}H^+}$, and $\Delta H_{ads\text{-}H^+}$, QM/MM activation barriers for individual C−C bonds, and additional derivations referenced in the text. The Supporting Information is available free of charge on the ACS Publications website at DOI: 10.1021/acs.jpcc.5b01715.

■ AUTHOR INFORMATION

Corresponding Author

*(A.T.B.) E-mail: bell@cchem.berkeley.edu.

Notes

The authors declare no competing financial interest.

■ ACKNOWLEDGMENTS

This work was carried out with financial support from Chevron Energy Technology Co. and an NDSEG fellowship awarded by the American Society for Engineering Education. The CBMC simulations were carried out using resources of the National Energy Research Scientific Computing Center, a DOE Office of Science User Facility supported by the Office of Science of the U.S. Department of Energy (Contract DE-AC02-05CH11231), and the Center for Gas Separations Relevant to Clean Energy Technologies, an Energy Frontier Research Center funded by

DOI: 10.1021/acs.jpcc.5b01715
J. Phys. Chem. C 2015, 119, 10427−10438

the U.S. Department of Energy, Office of Science, Office of Basic Energy Sciences (Award DE-SC0001015).

REFERENCES

(1) Corma, A. Inorganic Solid Acids and Their Use in Acid-Catalyzed Hydrocarbon Reactions. *Chem. Rev.* **1995**, *95*, 559−614.
(2) Haag, W. O.; Dessau, R. M. Duality of Mechanism for Acid-Catalyzed Paraffin Cracking. *Proceedings − International Congress on Catalysis*, 8th; Verlag Chemie: Berlin, Germany, 1984; Vol. 2, pp 305−316.
(3) Kotrel, S.; Knözinger, H.; Gates, B. C. The Haag−Dessau Mechanism of Protolytic Cracking of Alkanes. *Microporous Mesoporous Mater.* **2000**, *35*−*36*, 11−20.
(4) Konno, H.; Okamura, T.; Kawahara, T.; Nakasaka, Y.; Tago, T.; Masuda, T. Kinetics of *n*-Hexane Cracking over ZSM-5 Zeolites − Effect of Crystal Size on Effectiveness Factor and Catalyst Lifetime. *Chem. Eng. J. (Amsterdam, Neth.)* **2012**, *207*−*208*, 490−496.
(5) Voogd, P.; van Bekkum, H. Limitation of *n*-Hexane and 3-Methylpentane Conversion over Zeolite ZSM-5 by Intracrystalline Diffusion. *Appl. Catal.* **1990**, *59*, 311−331.
(6) Haag, W. O.; Lago, R. M.; Weisz, P. B. Transport and Reactivity of Hydrocarbon Molecules in a Shape-Selective Zeolite. *Faraday Discuss. Chem. Soc.* **1982**, *72*, 317−330.
(7) Bučko, T.; Benco, L.; Dubay, O.; Dellago, C.; Hafner, J. Mechanism of Alkane Dehydrogenation Catalyzed by Acidic Zeolites: Ab Initio Transition Path Sampling. *J. Chem. Phys.* **2009**, *131*, No. 214508, DOI: 10.1063/1.3265715.
(8) Bučko, T.; Hafner, J. Entropy Effects in Hydrocarbon Conversion Reactions: Free-energy Integrations and Transition Path Sampling. *J. Phys.: Condens. Matter* **2010**, *22*, No. 384201, DOI: 10.1088/0953-8984/22/38/384201.
(9) Bučko, T.; Benco, L.; Hafner, J.; Ángyán, J. G. Monomolecular Cracking of Propane over Acidic Chabazite: An Ab Initio Molecular Dynamics and Transition Path Sampling Study. *J. Catal.* **2011**, *279*, 220−228.
(10) Zimmerman, P. M.; Tranca, D. C.; Gomes, J.; Lambrecht, D. S.; Head-Gordon, M.; Bell, A. T. Ab Initio Simulations Reveal that Reaction Dynamics Strongly Affect Product Selectivity for the Cracking of Alkanes over H-MFI. *J. Am. Chem. Soc.* **2012**, *134*, 19468−19476.
(11) Swisher, J. A.; Hansen, N.; Maesen, T.; Keil, F. J.; Smit, B.; Bell, A. T. Theoretical Simulation of *n*-Alkane Cracking on Zeolites. *J. Phys. Chem. C* **2010**, *114*, 10229−10239.
(12) Janda, A.; Bell, A. T. Effects of Si/Al Ratio on the Distribution of Framework Al and on the Rates of Alkane Monomolecular Cracking and Dehydrogenation in H-MFI. *J. Am. Chem. Soc.* **2013**, *135*, 19193−19207.
(13) Gounder, R.; Iglesia, E. Catalytic Consequences of Spatial Constraints and Acid Site Location for Monomolecular Alkane Activation on Zeolites. *J. Am. Chem. Soc.* **2009**, *131*, 1958−1971.
(14) van Bokhoven, J. A.; Williams, B. A.; Ji, W.; Koningsberger, D. C.; Kung, H. H.; Miller, J. T. Observation of a Compensation Relation for Monomolecular Alkane Cracking by Zeolites: The Dominant Role of Reactant Sorption. *J. Catal.* **2004**, *224*, 50−59.
(15) Tranca, D. C.; Hansen, N.; Swisher, J.; Smit, B.; Keil, F. J. Combined Density Functional Theory and Monte Carlo Analysis of Monomolecular Cracking of Light Alkanes over H-ZSM-5. *J. Phys. Chem. C* **2012**, *116*, 23408−23417.
(16) Myers, A. L.; Monson, P. A. Physical Adsorption of Gases: The Case for Absolute Adsorption as the Basis for Thermodynamic Analysis. *Adsorption* **2014**, *20*, 591−622.
(17) Dubbeldam, D.; Calero, S.; Vlugt, T. J. H.; Krishna, R.; Maesen, T. L. M.; Smit, B. United Atom Force Field for Alkanes in Nanoporous Materials. *J. Phys. Chem. B* **2004**, *108*, 12301−12313.
(18) Wood, G. B.; Panagiotopoulos, A. Z.; Rowlinson, J. S. Adsorption of Fluids in Model Zeolite Cavities. *Mol. Phys.* **1988**, *63*, 49−63.
(19) Smit, B.; Siepmann, I. J. Computer Simulations of the Energetics and Siting of *n*-Alkanes in Zeolites. *J. Phys. Chem.* **1994**, *98*, 8442−8452.
(20) Bhan, A.; Gounder, R.; Macht, J.; Iglesia, E. Entropy Considerations in Monomolecular Cracking of Alkanes on Acidic Zeolites. *J. Catal.* **2008**, *253*, 221−224.
(21) Eder, F.; Lercher, J. A. On the Role of the Pore Size and Tortuosity for Sorption of Alkanes in Molecular Sieves. *J. Phys. Chem. B* **1997**, *101*, 1273−1278.
(22) Eder, F.; Stockenhuber, M.; Lercher, J. A. Brønsted Acid Site and Pore Controlled Siting of Alkane Sorption in Acidic Molecular Sieves. *J. Phys. Chem. B* **1997**, *101*, 5414−5419.
(23) Donaldson, D. J.; Ammann, M.; Bartels-Rausch, T.; Pöschl, U. Standard States and Thermochemical Kinetics in Heterogeneous Atmospheric Chemistry. *J. Phys. Chem. A* **2012**, *116*, 6312−6316.
(24) Conway, B. E.; Angerstein-Kozlowska, H.; Dhar, H. P. On Selection of Standard States in Adsorption Isotherms. *Electrochim. Acta* **1974**, *19*, 455−460.
(25) Zelenay, P.; Habib, M. A.; Bockris, J. O. Adsorption from Solution on Platinum: An in Situ FTIR and Radiotracer Study. *Langmuir* **1986**, *2*, 393−405.
(26) Savara, A.; Schmidt, C. M.; Geiger, F. M.; Weitz, E. Adsorption Entropies and Enthalpies and Their Implications for Adsorbate Dynamics. *J. Phys. Chem. C* **2009**, *113*, 2806−2815.
(27) Savara, A. Standard States for Adsorption on Solid Surfaces: 2D Gases, Surface Liquids, and Langmuir Adsorbates. *J. Phys. Chem. C* **2013**, *117*, 15710−15715.
(28) Everett, D. H. The Thermodynamics of Adsorption Part II. Thermodynamics of Monolayers on Solids. *Trans. Faraday Soc.* **1950**, *46*, 942−957.
(29) Dubbeldam, D.; Calero, S.; Vlugt, T. J. H.; Krishna, R.; Maesen, T. L. M.; Beerdsen, E.; Smit, B. Force Field Parametrization through Fitting on Inflection Points in Isotherms. *Phys. Rev. Lett.* **2004**, *93*, No. 088302.
(30) De Moor, B. A.; Reyniers, M.-F.; Gobin, O. C.; Lercher, J. A.; Marin, G. B. Adsorption of C2-C8 *n*-Alkanes in Zeolites. *J. Phys. Chem. C* **2011**, *115*, 1204−1219.
(31) Martin, M. G.; Siepmann, J. I. Transferable Potentials for Phase Equilibria. 1. United-Atom Description of *n*-Alkanes. *J. Phys. Chem. B* **1998**, *102*, 2569−2577.
(32) van Koningsveld, H.; van Bekkum, H.; Jansen, J. C. On the Location and Disorder of the Tetrapropylammonium (TPA) Ion in Zeolite ZSM-5 with Improved Framework Accuracy. *Acta Crystallogr., Sect. B: Struct. Crystallogr. Cryst. Chem.* **1987**, *B43*, 127−132.
(33) Eder, F.; Lercher, J. A. Alkane Sorption in Molecular Sieves: The Contribution of Ordering, Intermolecular Interactions, and Sorption on Brønsted Acid Sites. *Zeolites* **1997**, *18*, 75−81.
(34) Jiang, T.; Göltl, F.; Bulo, R. E.; Sautet, P. Effect of Temperature on the Adsorption of Short Alkanes in the Zeolite SSZ-13: Adapting Adsorption Isotherms to Microporous Materials. *ACS Catal.* **2014**, *4*, 2351−2358.
(35) Sharada, S. M.; Zimmerman, P. M.; Bell, A. T.; Head-Gordon, M. Insights into the Kinetics of Cracking and Dehydrogenation Reactions of Light Alkanes in H-MFI. *J. Phys. Chem. C* **2013**, *117*, 12600−12611.
(36) Ding, B.-J.; Huang, S.-P.; Wang, W.-C. *n*-Butane Monomolecular Cracking on Acidic Zeolites: A Density Functional Study. *Chin. J. Chem.* **2008**, *26*, 1173−1180.
(37) Zimmerman, P. M.; Head-Gordon, M.; Bell, A. T. Selection and Validation of Charge and Lennard-Jones Parameters for QM/MM Simulations of Hydrocarbon Interactions with Zeolites. *J. Chem. Theory Comput.* **2011**, *7*, 1695−1703.
(38) Li, Y.-P.; Gomes, J.; Sharada, S. M.; Bell, A. T.; Head-Gordon, M. Improved Force-Field Parameters for QM/MM Simulations of the Energies of Adsorption for Molecules in Zeolites and a Free Rotor Correction to the Rigid Rotor Harmonic Oscillator Model for Adsorption Enthalpies. *J. Phys. Chem. C* **2015**, *119*, 1840−1850.
(39) Shao, Y.; Gan, Z.; Epifanovsky, E.; Gilbert, A. T. B.; Wormit, M.; Kussmann, J.; Lange, A. W.; Behn, A.; Deng, J.; Feng, X.; et al.

DOI: 10.1021/acs.jpcc.5b01715
J. Phys. Chem. C 2015, 119, 10427−10438

Advances in Molecular Quantum Chemistry Contained in the Q-Chem 4 Program Package. *Mol. Phys.* **2015**, *113*, 184−215.
(40) Chai, J.-D.; Head-Gordon, M. Systematic Optimization of Long-Range Corrected Hybrid Density Functionals. *J. Chem. Phys.* **2008**, *128*, No. 084106, DOI: 10.1063/1.2834918.
(41) Chai, J.-D.; Head-Gordon, M. Long-Range Corrected Hybrid Density Functionals with Damped Atom−Atom Dispersion Corrections. *Phys. Chem. Chem. Phys.* **2008**, *10*, 6615−6620.
(42) Krishnan, R.; Binkley, J. S.; Seeger, R.; Pople, J. A. Self-Consistent Molecular Orbital Methods. XX. A Basis Set for Correlated Wave Functions. *J. Chem. Phys.* **1980**, *72*, 650−654.
(43) Behn, A.; Zimmerman, P. M.; Bell, A. T.; Head-Gordon, M. Efficient Exploration of Reaction Paths via a Freezing String Method. *J. Chem. Phys.* **2011**, *135*, No. 224108, DOI: 10.1063/1.3664901.
(44) Sharada, S. M.; Zimmerman, P. M.; Bell, A. T.; Head-Gordon, M. Automated Transition State Searches without Evaluating the Hessian. *J. Chem. Theory Comput.* **2012**, *8*, 5166−5174.
(45) Baker, J. An Algorithm for the Location of Transition States. *J. Comput. Chem.* **1986**, *7*, 385−395.
(46) De Moor, B. A.; Ghysels, A.; Reyniers, M.-F.; Van Speybroeck, V.; Waroquier, M.; Marin, G. B. Normal Mode Analysis in Zeolites: Toward an Efficient Calculation of Adsorption Entropies. *J. Chem. Theory Comput.* **2011**, *7*, 1090−1101.
(47) Piccini, G. M.; Sauer, J. Quantum Chemical Free Energies: Structure Optimization and Vibrational Frequencies in Normal Modes. *J. Chem. Theory Comput.* **2013**, *9*, 5038−5045.
(48) Grimme, S. Supramolecular Binding Thermodynamics by Dispersion-Corrected Density Functional Theory. *Chem.−Eur. J.* **2012**, *18*, 9955−9964.
(49) Foster, M. D.; Rivin, I.; Treacy, M. M. J.; Delgado Friedrichs, O. A Geometric Solution to the Largest-Free-Sphere Problem in Zeolite Frameworks. *Microporous Mesoporous Mater.* **2006**, *90*, 32−38.
(50) Everett, D. H. The Thermodynamics of Adsorption Part III. Analysis and Discussion of Experimental Data. *Trans. Faraday Soc.* **1950**, *46*, 957−969.
(51) Zhu, W.; Kapteijn, F.; Moulijn, J. A. Adsorption of Light Alkanes on Silicalite-1: Reconciliation of Experimental Data and Molecular Simulations. *Phys. Chem. Chem. Phys.* **2000**, *2*, 1989−1995.
(52) June, L. R.; Bell, A. T.; Theodorou, D. N. Molecular Dynamics Studies of Butane and Hexane in Silicalite. *J. Phys. Chem.* **1992**, *96*, 1051−1060.
(53) Bates, S. P.; van Well, W. J. M.; van Santen, R. A. Location and Conformation of *n*-Alkanes in Zeolites: An Analysis of Configurational-Bias Monte Carlo Calculations. *J. Phys. Chem.* **1996**, *100*, 17573−17581.
(54) June, L. R.; Bell, A. T.; Theodorou, D. N. Prediction of Low Occupancy Sorption of Alkanes in Silicalite. *J. Phys. Chem.* **1990**, *94*, 1508−1516.
(55) Savitz, S.; Siperstein, F.; Gorte, R. J.; Myers, A. L. Calorimetric Study of Adsorption of Alkanes in High-Silica Zeolites. *J. Phys. Chem. B* **1998**, *102*, 6865−6872.
(56) Drain, L. E. Recent Studies of the Thermodynamics of Physical Adsorption. *Sci. Prog. (London, U. K.)* **1954**, *42*, 608−628.
(57) Eder, F.; He, Y.; Nivarthy, G.; Lercher, J. A. Sorption of Alkanes on Novel Pillared Zeolites; Comparison Between MCM-22 and MCM-36. *Recl. Trav. Chim. Pays-Bas* **1996**, *115*, 531−535.
(58) Han, O. H.; Kim, C. S.; Hong, S. B. Direct Evidence for the Nonrandom Nature of Al Substitution in Zeolite ZSM-5: An Investigation by ^{27}Al MAS and MQ MAS NMR. *Angew. Chem., Int. Ed. Engl.* **2002**, *41*, 469−472.
(59) Dědeček, J.; Kaucký, D.; Wichterlová, B. Co^{2+} Ion Siting in Pentasil-Containing Zeolites, Part 3. Co^{2+} Ion Sites and Their Occupation in ZSM-5: A VIS Diffuse Reflectance Spectroscopy Study. *Microporous Mesoporous Mater.* **2000**, *35−36*, 483−494.
(60) Dědeček, J.; Kaucký, D.; Wichterlová, B. Al Distribution in ZSM-5 Zeolites: An Experimental Study. *Chem. Commun. (Cambridge, U. K.)* **2001**, 970−971.
(61) Wichterlová, B.; Dědeček, J.; Sobalík, Z.; Čejka, J. Aluminium Distribution in High Silica Pentasil Ring Zeolites. *Stud. Surf. Sci. Catal.* **2001**, *135*, 344.
(62) Dědeček, J.; Kaucký, D.; Wichterlová, B.; Gonsiorová, O. Co^{2+} Ions as Probes of Al Distribution in the Framework of Zeolites. ZSM-5 Study. *Phys. Chem. Chem. Phys.* **2002**, *4*, 5406−5413.
(63) Dědeček, J.; Balgová, V.; Pashková, V.; Klein, P.; Wichterlová, B. Synthesis of ZSM-5 Zeolites with Defined Distribution of Al Atoms in the Framework and Multinuclear MAS NMR Analysis of the Control of Al Distribution. *Chem. Mater.* **2012**, *24*, 3231−3239.
(64) Sklenak, S.; Dědeček, J.; Li, C.; Wichterlová, B.; Gábová, V.; Sierka, M.; Sauer, J. Aluminum Siting in Silicon-Rich Zeolite Frameworks: A Combined High-Resolution ^{27}Al NMR Spectroscopy and Quantum Mechanics/Molecular Mechanics Study of ZSM-5. *Angew. Chem., Int. Ed.* **2007**, *46*, 7286−7289.
(65) Sklenak, S.; Dědeček, J.; Li, C.; Wichterlová, B.; Gábová, V.; Sierka, M.; Sauer, J. Aluminium Siting in the ZSM-5 Framework by Combination of High Resolution ^{27}Al NMR and DFT/MM Calculations. *Phys. Chem. Chem. Phys.* **2009**, *11*, 1237−1247.
(66) Dědeček, J.; Sobalík, Z.; Wichterlová, B. Siting and Distribution of Framework Aluminium Atoms in Silicon-Rich Zeolites and Impact on Catalysis. *Catal. Rev.: Sci. Eng.* **2012**, *54*, 135−223.
(67) Narbeshuber, T. F.; Vinek, H.; Lercher, J. A. Monomolecular Conversion of Light Alkanes over H-ZSM-5. *J. Catal.* **1995**, *157*, 388−395.
(68) Gounder, R.; Iglesia, E. The Roles of Entropy and Enthalpy in Stabilizing Ion-Pairs at Transition States in Zeolite Acid Catalysis. *Acc. Chem. Res.* **2012**, *45*, 229−238.

DOI: 10.1021/acs.jpcc.5b01715
J. Phys. Chem. C 2015, 119, 10427−10438